Photoprotons from Mo^{100} and Mo^{92}†

W. A. BUTLER* AND G. M. ALMY
Department of Physics, University of Illinois, Urbana, Illinois
(Received March 23, 1953)

The absolute yield and the energy and angular distributions of protons emitted from targets of concentrated isotopes Mo^{92} and Mo^{100}, under betatron x-ray radiation of maximum energy 22.5 Mev, have been determined with nuclear emulsions as detector of protons.

For Mo^{92} the proton is less tightly bound than the neutron by 5.0 Mev; for Mo^{100} the proton is more tightly bound by 2.4 Mev. Comparison of the large yield and the energy distribution of protons from Mo^{92} with those calculated from the statistical model shows good agreement except for an observed excess of high energy protons, which are also anisotropic. They are presumably due to a direct emission process with which neutron emission does not compete in the normal way.

With Mo^{100}, however, the yield, though 20 times smaller, exceeds the yield predicted on the statistical model by 20 to 125 times depending upon the processes and parameters assumed in the calculation. Most of the protons, therefore, must come from a direct process. The observed energy distribution is similar to one computed using the experimental (γ, p) cross section if it is assumed that the residual nucleus is left with a typical exponential energy level density distribution. The angular distribution is strongly anisotropic with a maximum near 45°, for protons of energy greater than 5 Mev.

A NUMBER of experiments on the (γ, p) process in medium weight nuclei have indicated the occurrence of a direct photoproton process in addition to the normal competitive emission of protons and neutrons from an excited statistical model or compound nucleus, calculated according to Weisskopf and Ewing.[1] Hirzel and Wäffler[2] found from activities induced by the 17.6-Mev Li γ-ray that the cross sections of (γ, p) processes relative to (γ, n) were much greater than calculated. In silver[3] and copper,[4,5] on the other hand, the ratio of total yield of protons to neutrons ejected by 20-Mev betatron x-rays is in satisfactory agreement with prediction. For these elements, and in Rh,[6] the evidence for a direct process is that the observed proton energy spectrum rises definitely above the theoretical spectrum at high proton energies and just these protons show a pronounced departure from spherical symmetry in angular distribution. As another example of departure from the expectations based on the statistical model, Wilkinson and Carver[7] have found that the yield of photoprotons from A^{40}, irradiated with Li γ-rays, is several times the predicted yield. The proton energy distribution is, in the main, similar to that expected from a statistical model.

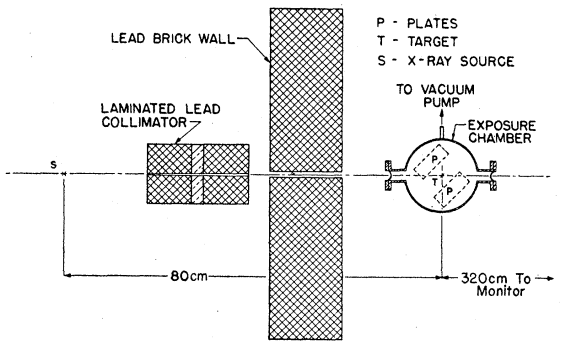

FIG. 1. Experimental arrangement. Collimated x-rays from betatron source S pass through target T and on to monitor. Protons are caught in four plates P arranged in pairs above and below the beam.

Levinger and Bethe[8] and Courant,[9] in their papers on dipole absorption in nuclei, have tentatively proposed a picture of the photonuclear process. It is suggested that in the absorption of the photon only a small part of the nucleus, perhaps only a single proton, is involved. Following absorption a proton may be emitted before a statistical distribution of the excitation energy and normal competition between neutron and proton emission is established. The initial or direct emission of protons is presumably responsible for the excess of high energy anisotropic protons observed in Ag, Cu, and Rh. In cases where the total proton yield, though small, greatly exceeds the yield calculated on the basis of the statistical model the direct process may account for nearly all of the emitted protons.

It therefore becomes of interest to determine the characteristics of the photon-protons in a case where they must be mainly ascribed to the direct process. The work of Duffield, Hsiao, and Sloth[10] has revealed that Mo^{100} is a good nucleus for this purpose. They have shown that the (γ, p) reaction, as well as (γ, n), leads to a radioactive nucleus and that the ratio $\sigma(\gamma, p)/\sigma(\gamma, n)$ is about 100 times that predicted from the statistical model in the range 16 to 19 Mev. They have

† Assisted by the Joint Program of the U. S. Office of Naval Research and the U. S. Atomic Energy Commission.
* Now at Carleton College, Northfield, Minnesota.
[1] V. F. Weisskopf and D. H. Ewing, Phys. Rev. **57**, 472 (1940).
[2] O. Hirzel and H. Wäffler, Helv. Phys. Acta **20**, 373 (1947); see A. Paskin, Phys. Rev. **87**, 197 (1952).
[3] B. C. Diven and G. M. Almy, Phys. Rev. **80**, 407 (1950).
[4] P. R. Byerley, Jr., and W. E. Stephens, Phys. Rev. **83**, 54 (1951).
[5] Mann, Halpern, and Rothman, Phys. Rev. **87**, 146 (1952).
[6] Curtis, Hornbostel, Lee, and Salant, Phys. Rev. **77**, 290 (1951).
[7] D. H. Wilkinson and J. H. Carver, Phys. Rev. **83**, 466 (1951).
[8] J. S. Levinger and H. Bethe, Phys. Rev. **78**, 115 (1950).
[9] E. D. Courant, Phys. Rev. **82**, 703 (1951).
[10] Duffield, Hsiao, and Sloth, Phys. Rev. **79**, 1011 (1950); E. N. Sloth, Master's thesis, University of Illinois, 1950 (unpublished).

also shown that the binding energy of a proton in Mo^{100} is greater than that of a neutron by 2.4 Mev in contrast to Ag, Cu, and Rh where the proton is less tightly bound by a few Mev. It is this difference in the relative thresholds of proton and neutron emission that leads to a much wider predicted variation in numbers of protons, on the basis of the statistical model, than is observed.

The principal purposes of the present investigation are the direct observation of the protons from Mo^{100}, the determination of their absolute yield, their distribution in energy and angle and a comparison of their yield and energy spectrum with theoretical expectations based on various assumptions as to the processes occurring.

As a comparison experiment a parallel study has been made of Mo^{92}. In this case, the proton is 5 Mev less tightly bound than the neutron. It is therefore expected that, as in Ag and Cu, the yield and the energy and angular distributions will be in agreement with statistical model calculations except for deviations at high proton energies. Unpublished data on the (γ, n) cross section of Mo^{92}, essential to the comparison with theory, have been generously provided by Katz.[11]

EXPERIMENTAL PROCEDURES AND RESULTS

The experimental arrangement is shown in Fig. 1. X-rays from the betatron source with a maximum energy of 22.5 Mev for all of the exposures were collimated with lead to a pencil of angular diameter 0.012 radian or a lateral diameter of 1.0 cm at the Mo target T, 80 cm from the x-ray source. The target was mounted in the center of a cylindrical exposure chamber. The x-rays entered and left through 0.002-in. aluminum windows. The plates P were mounted in pairs, one above and one below the beam, sensitive surfaces separated by 1.80 cm. Ilford type C-2, 200 micron emulsions were used throughout. During runs the chamber was evacuated and filled with water vapor to a pressure of about 16 mm Hg. An electromagnet with pole pieces mounted inside the chamber provided a field for deflecting the slower Compton electrons from the plates.

The concentrated isotopes, Mo^{100} and Mo^{92}, were obtained from Oak Ridge as oxides. They were reduced almost quantitatively to the metal by holding them in a hydrogen atmosphere for one hour at 525°C and another hour at 1000°C. The metal granules were pulverized or flattened and attached with thinned zapon to Nylon films which weighed approximately 0.2 mg/cm².

The weights of the Mo isotopes present were checked by intercomparison of the activities of simultaneously irradiated targets of Mo^{92} and Mo^{100} and a sample of natural Mo similarly reduced from the oxide and mounted. The natural abundance of the isotopes was taken from Hibbs.[12] It was determined that the Mo^{92} target, which weighed 23.6 mg, contained 21.6 mg of Mo^{92}. The Mo^{100} target weighed approximately 13 mg and contained 10.9 mg of Mo^{100} and 0.21 mg of Mo^{92}. The Mo^{92} impurity in the Mo^{100} target was determined with care since it yields a substantial background of protons in the Mo^{100} plates.

TABLE I. Exposures selected for study.

X-ray target	Roentgens on target	$\bar{\phi}$*	Area searched in mm²	Number of tracks observed with energies >3 Mev
Mo^{92}	8000	24°	17.29	468
		90°	35.11	1089
		156°	17.60	477
Mo^{100}	8262	29°	170.7	191
		44.5°	171.4	237
		90°	561.7	711
		135.5°	170.7	210
		151°	172.4	190
Background (Nylon films)	6075	29°	172.5	12
		44.5°	173.0	20
		90°	573.7	41
		135.5°	173.2	14
		151°	175.6	18

* ϕ is the average value of ϕ, the angle between the x-ray beam and the protons, for the plate area scanned.

In each target the average density of metal was about 17 mg/cm². The Mo^{100} target was more than covered by the x-ray beam, but only 90 percent of the Mo^{92} target was covered.

The x-ray beam was monitored with a Victoreen thimble mounted in an Al block whose faces were 4 cm from the thimble. The front face was 400 cm from the x-ray source. The response of this monitor had been calculated according to Fowler, Lauritsen, and Lauritsen.[13] Assuming that the x-rays are described by the Schiff forward spectrum, tables were constructed giving the number of quanta per cm² per Mev interval per roentgen, falling on the surface of the Al block.

To check against accidental variations in the primary Victoreen thimble, a second thimble was placed in the block a short distance behind the first. As a second check on the integrated x-ray flux a tantalum disk (0.005×0.83 in.) was placed on the front face of the Al block in each run and the induced activity per gram (8.2-hour) taken as a relative measure of the total flux per unit area, maximum energy held constant. The relative readings of the three monitors agreed within a few percent in the runs from which plates were used.

Since the Mo target and monitor face were 80 cm and 400 cm, respectively, from the x-ray source the flux per cm² on the target was taken as 25 times that on the monitor. To check this, a comparison was made of the activities per g of two simultaneously irradiated tan-

[11] See R. Montalbetti and L. Katz, Phys. Rev. **83**, 892 (1951) for preliminary results.

[12] R. F. Hibbs, Oak Ridge National Laboratory Report AECU-556, 1949 (unpublished).

[13] Fowler, Lauritsen, and Lauritsen, Revs. Modern Phys. **20**, 263 (1948).

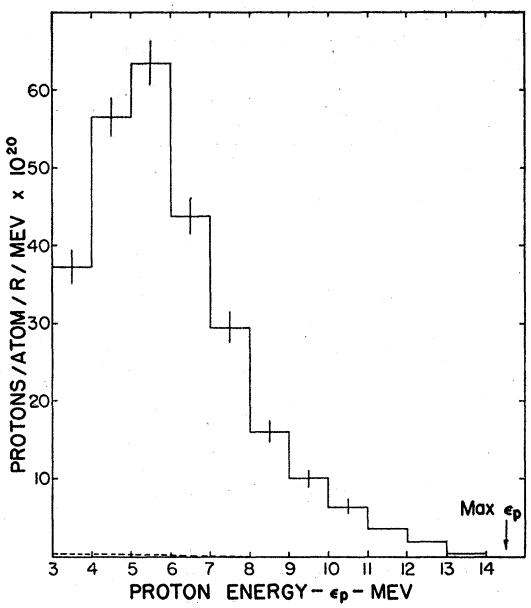

FIG. 2. Energy spectrum of photoprotons from Mo^{92} under 22.5-Mev bremsstrahlung. Dashed line is background. Max $\epsilon_p = 22.5 - B_p = 14.5$ Mev. Vertical lines show statistical uncertainties.

talum samples, each 0.005 in. thick, one shaped like the target and at the target position, the other on the monitor face. In two runs the ratios of specific activities were 25.1 and 25.9.

The nuclear plates were processed and read with standard techniques. The exposures selected for study are listed in Table I, which also gives the angles selected, areas searched, and numbers of proton tracks. Calculation showed that by combining the numbers of tracks on corresponding areas of upper and lower plates errors in the number per unit solid angle due to size, orientation or lack of uniformity of the target or to lack of symmetry of the x-ray beam above and below the midplane of the plate assembly could not exceed a few percent.

Range in emulsion and angle to the beam were determined for each track originating in the emulsion surface (2μ resolution) within predetermined swaths. The energy lost by a proton in the emulsion was determined from curves plotted from data in the literature.[14] To this energy was added the energy loss in the Mo-Nylon target; it was assumed that the proton came from the central plane of the target. The loss in the water vapor was negligible. The uncertainty in this increment is thus equal to its magnitude which at the largest angle varied from 0.7 Mev at a proton energy of 3 Mev to 0.25 Mev at 13 Mev. The few protons which emerged at the bottom or top of the emulsion were each assigned the average energy of all protons of longer range.

[14] Lattes, Fowler, and Cüer, Proc. Phys. Soc. (London) **59**, 883 (1947); Bradner, Smith, Barkas, and Bishop, Phys. Rev. **77**, 462 (1950).

The background exposure plates (Table I) were read in all regions used in the Mo plates. The total background correction was less than 1 percent for Mo^{92} but about 10 percent of the low yield from Mo^{100}. There was, in addition, a larger correction to the Mo^{100} data due to the protons from Mo^{92}, which could be made at each energy and angle since the spectrum of Mo^{92} had been determined in detail.

The contribution of the small amounts of intermediate Mo isotopes to the observed protons from the Mo^{100} target was estimated. For this purpose the abundance analysis supplied by Oak Ridge, the neutron and proton thresholds determined experimentally or from an empirical mass formula[15] and the functions for the relative probability of neutron and proton emission from a statistical model, plotted by Feld *et al.*,[16,17] were used. The result was that the total contribution of statistical theory protons from intermediate isotopes was about 2.5 percent of the total protons observed on the Mo^{100} plates. No correction was made for these protons. Direct process protons should be roughly proportional to isotopic abundance and were also neglected. Background due to (n, p) processes in the target can be neglected.[3]

A numerical integration over all angles for each Mev energy interval of the number of proton per unit

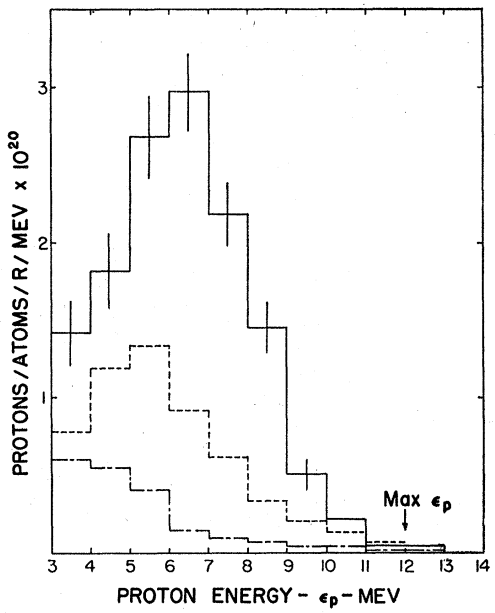

FIG. 3. Energy spectrum of photoprotons from Mo^{100} under 22.5-Mev bremsstrahlung. Backgrounds from run without Mo (lowest histogram) and from Mo^{92} impurity (middle histogram) have been subtracted to give net protons (upper histogram). Max $\epsilon_p = 22.5 - B_p = 12.0$ Mev. Vertical lines show statistical uncertainties.

[15] N. Metropolis and G. Reitwiesner, *Table of Atomic Masses* (1950).

[16] Feld, Feshbach, Goldberger, Goldstein, and Weisskopf, U.S. Atomic Energy Commission Report N-YO-636 (unpublished).

[17] J. M. Blatt and V. Weisskopf, *Theoretical Nuclear Physics* (John Wiley and Sons, Inc., New York, 1952), p. 373.

solid angle gave the total number of protons emitted in each energy interval. The results, with statistical errors, are given in Fig. 2 for Mo^{92} and in Fig. 3 for Mo^{100}. The backgrounds which have been subtracted are also shown.

The angular distributions are for the two isotopes plotted in Figs. 4 and 5. Estimates of multiple and large angle single scattering of protons in the target show that they would not affect the relatively flat distributions for Mo^{92} but may have an appreciable effect for Mo^{100}. The numbers of protons observed at the extreme angles (29° and 151°) are somewhat higher than they would be with a thinner target.

COMPARISON WITH THEORY

On the basis of the statistical model the energy distribution of the photoprotons can be expressed as follows:

$$F(\epsilon_p)=A\,\epsilon_p\sigma(\epsilon_p)\int_{B_p+\epsilon_p}^{E_{\max}}\frac{N(E)\sigma_\gamma(E)\omega(E_R)dE}{\sum_b\Gamma_b} \quad (1)$$

in which

$F(\epsilon_p)$ = absolute number of protons of energy ϵ_p per Mev interval per roentgen at the target per nucleus in the beam;

$\sigma_p(\epsilon_p)$ = reaction cross section for proton of energy ϵ_p on residual nucleus;

$N(E)$ = number of x-ray quanta per cm^2 per Mev interval per roentgen at the target, at x-ray energy E (Schiff forward spectrum);

$\sigma_\gamma(E)$ = cross section for absorption of quantum of energy E;

$\omega(E_R)$ = energy level density in residual nucleus with excitation energy $E_R=E-B_p-\epsilon_p$; $\omega=C\exp[2(aE_R)]^{\frac{1}{2}}$;

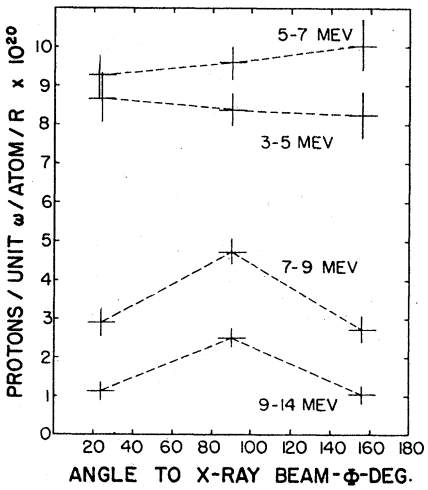

FIG. 4. Angular distribution of photoprotons from Mo^{92}. Horizontal lines are approximate angular intervals.

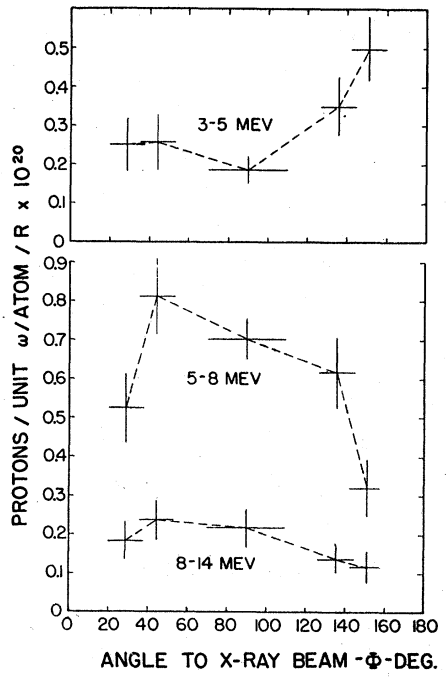

FIG. 5. Angular distribution of photoprotons from Mo^{100}. Horizontal lines are approximate angular intervals.

$\Gamma_b=A\int_0^{\epsilon_{b\max}}\epsilon_b\sigma_b(\epsilon_b)\omega(E_R)d\epsilon_b$, is the probability per unit time of the emission of a particle b. It is a function of E since $E_R=E-B_b-\epsilon_b$ and $\epsilon_{b\max}=E-B_b$;

B_b = binding energy of particle b;

A = a constant, independent of energy. It depends upon the mass of the escaping particle but will be taken the same for neutrons and protons, the only particles for which Γ_b is large enough to be considered here. It therefore cancels out in Eq. (1).

Since $\sigma_\gamma/\sum\Gamma_b=\sigma(\gamma,n)/\Gamma_n=\sigma(\gamma,p)/\Gamma_p$, the first of these equivalents can be replaced by one of the others in Eq. (1). $\sigma(\gamma,n)$ is the cross section usually known from experiment in which case the useful form of Eq. (1) is

$$F(\epsilon_p)=\epsilon_p\sigma_p(\epsilon_p)\int_{B_p+\epsilon_p}^{E_{\max}}\frac{N(E)\sigma(\gamma,n)\omega(E_R)dE}{\Gamma_n'}, \quad (2)$$

where $\Gamma_n'=\Gamma_n/A$. The integrals were evaluated numerically, with energy intervals of 1 Mev.

The neutron energy distribution can be calculated with an expression analogous to Eq. (2). The total number of neutrons or protons can be predicted by numerically integrating $F(\epsilon_n)$ or $F(\epsilon_p)$. The number of neutrons is also given by the integral of $\sigma(\gamma,n)N(E)$ from $E=B_n$ to $E=E_{\max}$.

Mo^{92}

This isotope, for which results similar to those in Cu, Rh, and Ag are to be expected, will be discussed

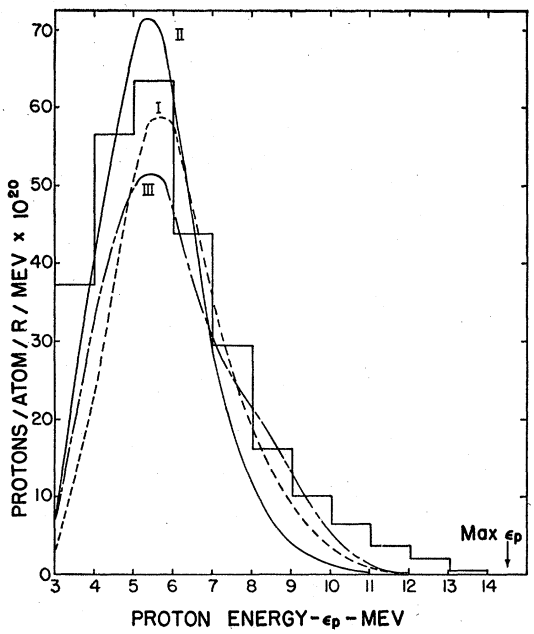

FIG. 6. Comparison of observed and calculated unnormalized proton energy spectra for Mo^{92}. Observed spectrum: histogram. Calculated spectra based on statistical model: $F(\epsilon_p)$ from Eq. (2), with $r_0=1.3\times10^{-13}$ cm, and ω_1 for I, ω_2 for II, ω_2' for III (see text). III fits observed shape best. Observed spectrum shows excess of high energy protons which are anisotropic (Fig. 4) and probably due to a direct emission process.

first. The values and sources of parameters used in the calculation of $F(\epsilon_p)$ by Eq. (2) are as follows.

$\sigma(\gamma, n)$

This is the sum of two curves supplied by Katz,[11] deduced from the yields of positron activity from the two isomers of Mo^{91} excited by betatron x-rays. The half-lives are 15.5 min and 65.5 sec and the yield from the former is about five times the yield from the latter.

B_n and B_p

At Illinois[18] the threshold for the 15.5-min activity was found to be 13.28 ± 0.15 Mev; Katz found 13.2 ± 0.1 Mev. He also found 13.1 ± 0.1 Mev for the 65.5-sec activity and this is taken as the best measure of B_n.

The end point of the positron spectrum of the 15.5-min activity is 3.7 ± 0.1 Mev according to Duffield and Knight;[19] it is 3.32 ± 0.05 Mev according to Katz's more elaborate analysis. Using the latter value and assuming that positron emission of this energy leads to the ground state of Nb^{91}, $B_p-B_n=5.1$ Mev or $B_p=8.0$ Mev. B_p cannot be larger though an elucidation of the decay scheme of Mo^{91} might lead to a lower value. For convenience in calculation B_n has been taken as 13.0 Mev, B_p as 8.0 Mev.

[18] Hanson, Duffield, Knight, Diven, and Palevsky, Phys. Rev. **76**, 578 (1949).
[19] R. B. Duffield and J. D. Knight, Phys. Rev. **76**, 573 (1949).

$\sigma_p(\epsilon_p)$ and $\sigma_n(\epsilon_n)$, r_0

Proton and neutron reaction cross sections were taken from Feld *et al.*,[16] or Blatt and Weisskopf[20] by graphical interpolation. Cross sections have been calculated for two values of the nuclear radius factor r_0, 1.3×10^{-13} cm and 1.5×10^{-13} cm.

$\omega(E_R)$

Proton energy distributions have been calculated with the following choices of $\omega(E_R)$:

1. $\omega_1=C\exp[2(2.85E_R)]^{\frac{1}{2}}$. This choice of the parameter $a=2.85$ corresponds for Mo to a value which proved to be satisfactory for Ag.[3]
2. $\omega_2=C\exp[2(5.3E_R)]^{\frac{1}{2}}$. The value $a=5.3$ was interpolated from values given for various nuclei by Blatt and Weisskopf.[21]
3. $\omega_2'=C\exp[2\times5.3(E_R-3)]^{\frac{1}{2}}$, for $E_R\geq4$ Mev;
   $=C\times10$, for $E_R\leq3$ Mev.

The last form of ω takes cognizance in a rough way of the general observation that the denstiy of levels increases more slowly than exponentially for the first few Mev. It will increase the number of higher energy particles at the expense of those of lower energy.

The range of parameters chosen, a in ω and r_0, are about the extremes of values generally used in the interpretation of nuclear reactions with a statistical nuclear model.

A comparison between the unnormalized experimental proton energy spectrum and those calculated from Eq. (2) is plotted in Fig. 6, for $r_0=1.3\times10^{-13}$ cm and the three choices of ω. The general result is that the absolute numbers of protons in each energy interval can be satisfactorily predicted with reasonable choices of nuclear parameters except that the observed spectrum shows an excess of high energy protons, as was found with Ag and Cu. The modification of $\omega(E_R)$

TABLE II. Total yield of neutrons and protons from Mo^{92}. $E_{max}=22.5$ Mev, $B_n=13.0$ Mev, $B_p=8.0$ Mev.

		Protons atom^{-1} r^{-1} $\times10^{20}$ 3–14 Mev	Neutrons atom^{-1} r^{-1} $\times10^{20}$ 0–9.5 Mev
Observed		269±20	650±200
From $\sigma(\gamma, n)$ (Katz): $\int\sigma(\gamma, n)N(E)dE$			435
Calculated from statistical model, Eq. (2)			
$r_0\times10^{13}$, cm			
ω_1	1.30	200	421
	1.50	328	421
ω_2	1.30	222	434
	1.50	376	434
ω_2'	1.30	204	426
	1.50	337	426

[20] Reference 16, pp. 348, 352.
[21] Reference 17, pp. 371–374.

which assumes it is constant up to $E_R=3$ Mev accounts for some but not all of this discrepancy. It gives a spectrum shaped most nearly like that observed.

There is also an excess of observed protons in the 3–4 Mev interval. It may arise from one or all of three uncertain factors: (1) lack of energy resolution in the steeply rising, low energy range, (2) the absence of neutron competition up to an x-ray energy of 13 Mev, the neutron threshold, (3) a contribution of deuterons, which is energetically possible.

It is seen in Fig. 4 that just the high energy protons exhibit angular anisotropy. Thus, Mo^{92} falls into the group of medium weight nuclei with $B_p<B_n$ in which the photoproton emission is satisfactorily accounted for on the basis of the statistical model, except for the deviations shown by high energy protons.

In Table II, the observed and calculated total numbers of protons and neutrons are given. The calculated numbers of protons for $r_0=1.5\times10^{-13}$, as well as for $r_0=1.3\times10^{-13}$ cm, are listed and the experimental number falls between them. Protons emitted in a direct process are of course not included in the calculated number. The yield of protons is of the same order of magnitude as the yield of neutrons and is the largest (γ, p) yield yet observed in any nucleus. The neutron competiion is held back by the unusually large neutron threshold for Mo^{92}, "magic" in neutrons.

The number of neutrons listed as observed is based on counts of the 15.5-minute activity in the target at the end of two runs in which protons were collected, augmented about 20 percent by an estimate of the number of neutrons corresponding to the 65-sec activity of the isomeric state. The elapsed time of a run was several times the lifetime with several on and off periods; in addition the uncertainty in absolute counting was ±25 percent. Hence the reliability of the number is low and it was considered preferable to use in Eq. (2) Katz's values of $\sigma(\gamma, n)$ without normalization to the observed number of neutrons. If the "observed" number of neutrons were used to normalize Katz's $\sigma(\gamma, n)$, all calculated yields of neutrons and protons would be increased by about 50 percent. The calculation of total neutrons by Eq. (2) gives back satisfactorily the number of neutrons put in, through $\sigma(\gamma, n)$ $N(E)$, which is a comforting check on the method. This comparison appears in the last column of Table II.

Mo^{100}

As stated in the introduction, it has been shown from relative induced activities that $\sigma(\gamma, p)/\sigma(\gamma, n)$ is about 100 times that expected on the basis of the statistical model. In this section the yield and energy distribution of the observed protons will be compared with expectations on various assumptions as to the process producing them.

Information on nuclear parameters was obtained from the following sources.

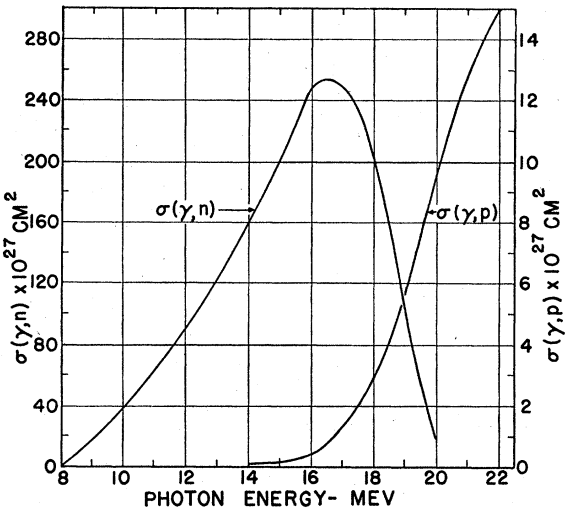

FIG. 7. $\sigma(\gamma, p)$ and $\sigma(\gamma, n)$ for Mo^{100}, obtained on relative scale by Duffield and Sloth. $\sigma(\gamma, p)$ normalized to observed number of protons. $\sigma(\gamma, n)$ normalized by absolute count of (γ, n) induced activity.

$\sigma(\gamma, n)$ and $\sigma(\gamma, p)$

Duffield and Sloth deduced the relative cross sections from the analysis of beta-activity *versus* betatron energy. For the present purpose, their yield curve for the (γ, p) process (leading to Nb^{99}, 2.5 min, $E_{\beta^-}=3.2$ Mev) was normalized to the directly observed yield of protons at 22.5 Mev and $\sigma(\gamma, p)$ was recalculated on an absolute basis. Their relative $\sigma(\gamma, n)$ curve was normalized with an absolute count of the 67-hour β-activity of Mo^{99} in the Mo^{100} target after runs in which protons were collected. The decay scheme of Mo^{99} has been established[22] and the lifetime of the counted activity is much greater than the elapsed time of the intermittent irradiation. Hence the principal uncertainty comes from errors in absolute counting which may amount to ±25 percent. $\sigma(\gamma, n)$ and $\sigma(\gamma, p)$ are shown in Fig. 7.

B_n and B_p

From the threshold of the (γ, n) induced activity Duffield has obtained $B_n=8.1$ Mev (unpublished). From the relation $B_p-B_n=E_{\beta^-}-(n-H)$, B_p was determined to be 10.5 Mev. The values used in calculations were $B_p=10.5$ Mev and $B_n=8.0$ Mev.

$\sigma_p(\epsilon_p)$, $\sigma_n(\epsilon_n)$, r_0, $\omega(E_R)$

Reaction cross sections, nuclear radius, and level density were chosen as described in the section on Mo^{92}. Calculations have been made only with ω_1.

The following calculations have been made for the theoretical proton energy distributions.

(1) *Calculation of $F(\epsilon_p)$ on basis of statistical model.*— The proton spectrum was calculated exactly as for

[22] M. E. Bunker and R. Canada, Phys. Rev. **80**, 961 (1950).

Mo^{92} from Eq. (2) using $\sigma(\gamma, n)$ from Fig. 7, $r_0=1.3\times10^{-13}$ cm and ω_1. It is plotted in Fig. 8, I. As expected from Duffield and Sloth's ratio of $\sigma(\gamma, p)/\sigma(\gamma, n)$, the total calculated yield of protons in the proton energy range 3–14 Mev is about 0.008 of the observed number.

(2) Calculation of $F(\epsilon_p)$ assuming a $(\gamma, 2n)$ process.[23] —The number of protons to be expected on the basis of the statistical model is increased if one assumes that a $(\gamma, 2n)$ process occurs with high probability when the energy of excitation in the initial residual (γ, n) nucleus (Mo^{99}) exceeds the threshold for emission of a neutron from that nucleus. In this case the experimental $\sigma(\gamma, n)$ corresponds to only a fraction of the processes in which an initial neutron is emitted from Mo^{100}, the remainder being $(\gamma, 2n)$. Consequently, the calculated number of competing (γ, p) processes is increased.

B_{2n} for Mo^{100} was taken from an empirical mass formula[15] to be 15 Mev, or B_n for Mo^{99} to be 7 Mev. As an extreme case, leading to the maximum calculated number of protons, it was assumed that whenever the excitation of the residual nucleus Mo^{99} exceeds 7 Mev a second neutron will be emitted. Hence, in Eq. (2), the limits of integration of ϵ_n are set at $\epsilon_n=E-15$ and $\epsilon_{n\max}=E-8$. With these assumptions and taking $r_0=1.30\times10^{-13}$ cm, the total number of protons between 3 and 14 Mev is increased by about threefold, to 0.027 of the observed number (Curve II, Fig. 8). If $r_0=1.5\times10^{-13}$ cm, this fraction is 0.046.

Thus the number of protons observed exceeds by 20 to 125 times the number calculated from the statistical model, depending upon the assumptions as to process and parameters. The photoprotons from Mo^{100} hence must arise mainly from a direct process in which normal competition with neutrons does not occur.

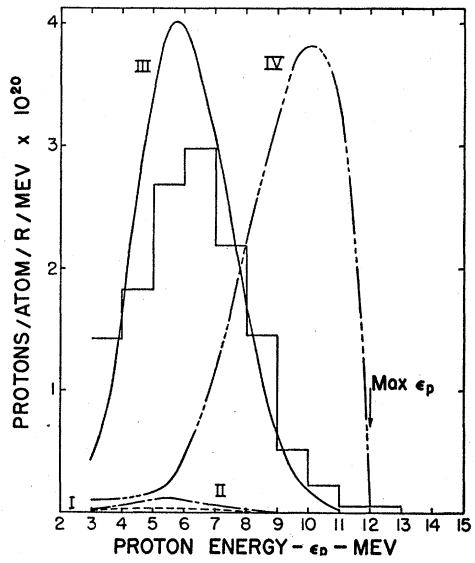

FIG. 8. Comparison of observed and calculated proton energy spectra from Mo^{100}. I (lowest curve) and II are based on the statistical model and account for only a small fraction of observed protons. III and IV make use of the experimental $\sigma(\gamma, p)$; IV assumes residual nucleus after emission of proton is left in ground state; III assumes residual nucleus with typical exponential energy distribution, ω_1.

[23] See L. Eyges, Phys. Rev. **86**, 325 (1952).

(3) Calculations of $F(\epsilon_p)$ based on $\sigma(\gamma, p)$.—$\sigma(\gamma, p)$ deduced from experimental data must reflect the actual photoproton processes. If this is mainly a direct emission before statistical distribution in the nucleus occurs, calculations based on the statistical model do not apply.

The direct process has sometimes been thought of as the excitation and ejection of a proton near the nuclear surface with the remainder of the nucleus relatively unexcited. The extreme assumption on this picture is that the residual nucleus is left in the ground state. In this case, $F(\epsilon_p)$ is simply $N(E)\sigma(\gamma, p)$, which is plotted in Fig. 8, IV. This distribution is greatly shifted to high energies from the actual distribution.

The opposite extreme assumption seems to account much better for the observed distribution, namely, that even in a direct emission, the energy states available in the residual nucleus have the usual exponential energy level distribution. In this case the probability of emission of a proton of energy ϵ_p from a single excited state E is given by

$$\epsilon_p\sigma_p(\epsilon_p)\omega(E-B_p-\epsilon_p)\Big/\int_0^{\epsilon_{p\max}}\epsilon_p\sigma_p(\epsilon_p)\omega(E_R)d\epsilon_p,$$

if the usual reaction cross section σ_p is assumed to apply to direct emission. Formally the calculation of $F(\epsilon_p)$ proceeds by Eq. (2) with $\sigma(\gamma, p)/\Gamma_p'$ replacing $\sigma(\gamma, n)/\Gamma_n'$. $F(\epsilon_p)$ so obtained is plotted unnormalized in Fig. 8, III, and is in satisfactory agreement with the observed spectrum. ω_1 and $r_0=1.30\times10^{-13}$ cm were used in the calculation. The agreement would be improved if ω were modified so as to remain constant from $E_R=0$ to $E_R=3$ Mev, as can be seen by comparing II and III in Fig. 6 for Mo^{92}.

The total observed yields of protons and neutrons are listed in Table III, together with the total yields of protons calculated in the ways described above.

The (γ, p) cross section for Mo^{100} has also been calculated on Courant's theory of a direct process[9] in which it is assumed that the photon is absorbed by a single proton in a suitable square-well nuclear potential and that the proton is then emitted through the usual Coulomb barrier without the formation of a compound nucleus. With the experimental proton binding energy and other parameters for Mo^{100} inserted, his expression for $\sigma(\gamma, p)$ leads to values only about 0.025 of that observed at photon energies of 20 to 22 Mev (Fig. 7). Thus, for Mo^{100}, $\sigma(\gamma, p)$ and the proton yield calculated on this basis are much less than observed and about the same as expected from the statistical model.

The angular distributions of photoprotons from Mo^{100} were plotted in Fig. 4. The large group between 5 and 8 Mev, comprising 55 percent of all protons are strongly anisotropic and peaked forward with a maxi-

mum near 45°. The steep drop at low and high angles indicates that the numbers near 0 and 180° are small, especially since multiple scattering in the target which is appreciable will tend to flatten the distribution. The smaller high energy group above 8 Mev shows within statistical errors the same distribution as the 5–8 Mev group.

Thus, nearly all of the protons of energy above 5 Mev show strong anisotropy roughly similar to that reported by Mann, Halpern, and Rothman[5] for the small anisotropic components in copper and cobalt in which most of the protons are accounted for on the statistical theory. The asymmetry about 90° implies interference between the wave functions, corresponding to different angular momenta, which describe the emitted protons.

The lower energy protons, 3–5 Mev, show an entirely different angular distribution. The numbers of protons per unit solid angle are approximately the same at 29°, 45°, and 90° but rise at 135° and 151°. The statistics are not very satisfactory, especially since the background of lower energy protons is comparable to the number from Mo^{100}. On the other hand, neither the background nor the Mo^{92} data taken from plates exposed under similar conditions showed any systematic excess of low energy protons in the backward direction. We have no suggestion as to how to account for the apparently anomalous distribution.

SUMMARY

The yield and energy and angular distributions of photoprotons from Mo^{92} for which $B_p=B_n-5$ Mev can be accounted for on the basis of the statistical model, except for the expected departures at high proton energy. On the other hand, the observed number of protons from Mo^{100}, for which $B_p=B_n+2.5$ Mev, exceeds the number expected on the statistical model by a factor of 20 to 125 depending upon the parameters and processes assumed in the calculation. The excess of protons requires a special assumption such as a direct process in which competition with neutron emission does not occur in the normal way. The proton energy distribution may be adequately described by a calculated distribution based on the observed $\sigma(\gamma, p)$ if it is assumed that the protons have the usual reaction cross section (Coulomb barrier) and that the energy levels available in the transition to the residual nucleus have a typical exponential level density. The observed yield of protons is also more than an order of magnitude greater than predicted on the basis of Courant's model for the direct emission of protons.

In angular distribution the protons from Mo^{100} with energies above 5 Mev are strongly anisotropic and unsymmetrical about 90°, with a maximum near 45° to the x-ray beam.

It is a pleasure to acknowledge the generous assistance of Robert A. Reitz during the runs with the betatron and the processing of the plates.

TABLE III. Total yield of protons and neutrons from Mo^{100}.

	Protons $atom^{-1}\,r^{-1}$ $\times10^{20}$ 3–12 Mev	Neutrons $atom^{-1}\,r^{-1}$ $\times10^{20}$ 0–14.5 Mev
Observed	13.4±1 (from tracks)	1180±300 (from activity)
$\int\sigma(\gamma, p)N(E)dE$	15.3	
Calculated:		$r_0\times10^{13}$, cm
(1) Statistical model, Eq. (2)	0.11	1.30
Using experimental $\sigma(\gamma, n)$, ω_1, assuming no $(\gamma, 2n)$ process	0.19	1.50
(2) Similar to (1), but assuming $(\gamma, 2n)$ process occurs	0.36 0.62	1.30 1.50
(3) Using experimental $\sigma(\gamma, p)$, ω_1 in Eq. (2)	14.8 15.0	1.30 1.50